International Journal of Reconfigurable and Embedded Systems (IJRES)
Vol. 11, No. 1, March 2022, pp. 59~70
ISSN: 2089-4864, DOI: 10.11591/ijres.v11.i1.pp59-70

Towards more accurate iris recognition system by using hybrid approach for feature extraction along with classifier

Arif Ullah[1], Abdu Salam[2], Hanane El Raoui[3], Dorsaf Sebai[4], Mahnaz Rafie[5]
[1]Faculty of Computer Science and Information Technology, Universiti Tun Hussein Onn Malaysia, Johor, Malaysia
[2]Department of Computer Science, Abdul Wali Khan University, Mardan, Pakistan
[3]Department of Computer Science and Artificial Intelligence, Universidad de Granada, Granada, Spain
[4]Cristal Laboratory, National School of Computer Sciences (ENSI), Manouba, Tunisia
[5] Department Computer Engineering, Islamic Azad University, Ramhormoz, Iran

Article Info

Article history:

Received Oct 10, 2021
Revised Jan 7, 2022
Accepted Jan 27, 2022

Keywords:

Classifier
Extraction
Feature
Hybrid
Iris

ABSTRACT

Iris recognition become one of the most accurate and reliable steadfast human biometric recognition system of the decad. This paper presents an accurate framework for iris recognition system using hybrid algorithm in preprocess and feature extraction section. The proposed model for iris recognition with significant feature extraction was divided into three main levels. First level is having pre-processing steps which are necessary for the desired tasks. Our model deploys on three types of datasets such as UBIRIS, CASIA, and MMU and gets optimal results for performing activity. At last, perform matching process with decision based classifier for iris recognition with acceptance or rejection rates. Experimental based results provide for analysis according to the false receipt rate and false refusal amount. In the third level, the error rate will be checked along with some statistical measures for final optimal results. Constructed on the outcome the planned method provided the most efficient effect as compared to the rest of the approach.

Corresponding Author:

Arif Ullah
Faculty of Computer Science and Information Technology, Universiti Tun Hussein Onn Malaysia
Beg Berkunci 101, Parit Raja, Johor 86400, Johor, Malaysia
Email: arifullahms88@gmail.com.

1. INTRODUCTION

In the current days, iris recognition as a functional feature of biometric is a chief biometric development. Human eye iris performances as substantial work in vast sympathy of a human being. The use of science and technology-based knowledge made an efficient effort in the field of biometrics authorization system where it used for individual can adapt it [1]. Biological science are used in different field for different purpose and the function of physiognomies are used for independence fingerprints, face and patterns, retina in iris system. Use of interactive physiognomies contemplate voice, handwritten autograph. One of the most reliable biometric is the iris, due to its stability, uniqueness and noninvasive nature [2]. Various extraction methods of iris features from iris image exist. The biometric authentication of iris image class schemes like local-global graph methodology, this is a graph based method for authentication of extracted features and many others for iris authentication need to be studied extensively. The existing schemes will be studied thoroughly and give experimental based results in order to have in-depth knowledge. This is because to have a state-owned of the art research for iris class recognition. Recognition in general and iris feature extraction is specific in security [2], [3].

2. RESEARCH METHOD

Methods for enhancing low contrast iris image class at preprocessing phase and significant features extraction process. This method for enhancing low contrast iris image class and significant features extraction through the proposed hybrid approach. For more information, the proposed technique working and explanation are present in Figure 1.

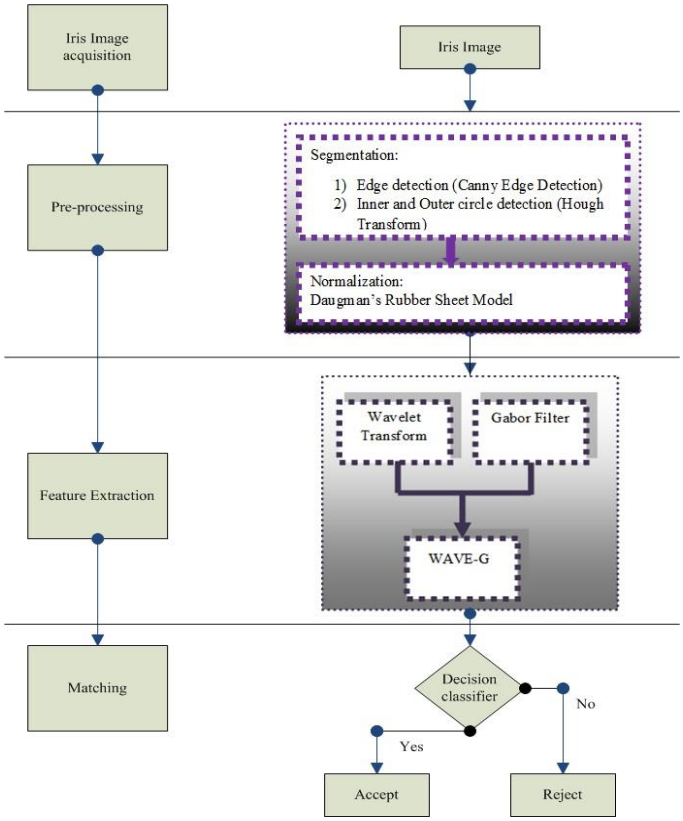

Figure 1. Iris recognition framework

Figure 1 shows the proposed model for iris recognition with significant feature extraction. This model divided into three main levels. First level is having pre-processing steps which are necessary for the desired tasks. Level one is further divided into two sub steps. We get iris image and start performing processing steps which first phase is segmentation where this step is consists of edge detection besides detecting the inward and external restrictions of the iris. In second level, select parameters for feature extraction then apply Gabor filter and wavelet transform and combined these two methods results according to the Haralick features scheme.

2.1. Wavelet: a suitable candidate for texture analysis

A near assessment of iris clone exposes the situation fertility in consistency. The grain material are sophisticated by the pendant. A portion since that, it involves of arbitrary distinguishings similar centrifugal stations, concentric channels, tincture points, and catacombs. These characteristics have unalike regularities, which canister is preeminent defined through a multi-determination inquiry (MRA) method [4], [5]. The remote wavelet change is MRA coordination, which dismiss brand the iris duplicate in unalike positioning plus vanquishing. Wavelet transmute is a multi-persistence performance, which consumes inductee effective demonstrations in numeral image allowance. The wild wavelet change is a precise algorithm intentional to chance a waveform or indicator in the spell domain into a cataloguing of measures grounded on an orthogonal source of unimportant determinate waves, or wavelets. These renovate dismiss be simply protracted to multidimensional signals, such as pictures, wherever the time sphere is traded through the interplanetary ground. It is consequential since a finitely fashioned, orthogonal MRA. In the bonds agreed there, one indicates a range scale J with test group rate of 2^J per unit pause, and strategies the specified

indicator *f* onto the planetary V_J; in theory by withdrawing the scalar produces. The procedure is reckless and has a low compactness gradation. The assembly adapts the assemblies to yield its iris piece codes [6], [7]. In direct division disengaged wavelet transmute [8]–[13]. The picture are essentially disintegrated i.e., separated into four sub-bands and unsympathetically sub-sampled by smearing detached wavelet convert as exposed in Figure 2. These sub-bands branded LH_1, HL_1, and HH_1 distinguish the supreme ruler wavelet measures i.e., aspect pictures whereas the sub-band LL_1 look like to grainy smooth amounts i.e., evaluation image. Towards gain the subsequent patchy near of wavelet quantities, the sub-band LL_1 unaided is added fragmented and frowningly investigated. These products in two-level wavelet disintegration as shown in Figure 2(b). Correspondingly, to accomplish auxiliary putrefaction, LL_2 will stand secondhand [14]. This extension remainders tray selected concluding sovereign is anxious. The integrities or deformed amounts in scheming and sub-band images are the essential assemblies, which stand revealed now as apposite aimed at surface examination and awareness. As palmtop-touches or function-surfaces need non-unbroken steely level dissimilarities, they are statistically patented by the structures in appraisal and aspect pictures. In additional words, the prices in the represent-posse images or their consolidations or the consequent structures from these ensembles distinctively explain a consistency. The structures grown after these wavelet rehabilitated images are shown to be used for consistency tagging [15]–[17].

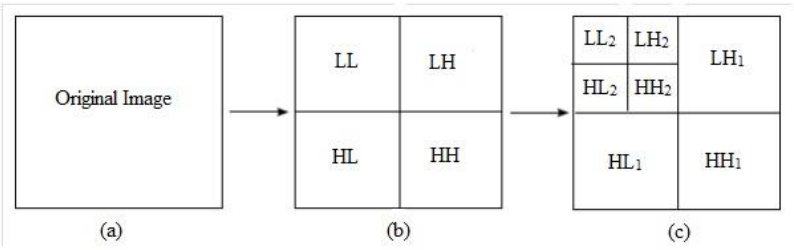

Figure 2. Two level decomposition by using discrete wavelet transform for (a) new image, (b) first section breakdown, and (c) second section breakdown [18]

2.2. Fast wavelet transform

The fast wavelet transform (FWT) is mathematical which is technique planned for the signal or wave. In the time range, it will convert obsessed by a sequence of measurements constructed scheduled an orthogonal basis of small finite waves or wavelets. The convert can be effortlessly protracted to multi-dimensional signals such as pictures. This algorithm was presented in [19], hypothetical base of this algorithm is to produce the orthogonal MRA finitely. The Mallat algorithm is an average method for distinct wavelet convert which is branded as a two-channel sub-group coder. Therefore, this conversion comprises of two parts as [20]: i) The disintegration procedure jumps with signal *s*, next determines the harmonizes of A_1 and D_1 and before persons of A_2 and D_2 and so on and ii) The renewal technique called the inverse detached wavelet transform starts from the manages of A_J and D_J next determines the organizes of A_{J-1} and then complete the synchronizes of A_{J-1} and D_{J-1} analyses individuals of A_{J-2} and so on [21]. In the multi-determination agenda, an orthogonal wavelet twitches through the ascending task φ then the wavelet purpose ψ. One of the essential relatives stands the identical-ruler relative which is defined in (1) and the wavelet function is in (2) as [22], [23].

$$\phi(x) = \sum_{k=-N}^{N}(w_n \phi(2x-k)) \quad (1)$$

$$\psi(x) = \sum_{k=-N}^{N}\left((-1)^k w_{1-k}\psi(2x-k)\right) \quad (2)$$

Altogether the filters used in dissimilar wavelet convert and inverse distinct wavelet changes are confidentially associated to the system given in (3) [24].

$$(w_n)_{n\in Z} \quad (3)$$

Obviously, if φ is trimly reinforced the arrangement w_n is determinate then canister be regarded as a filter. The strainer *w* which is called the clambering filter is having some belongings such as fixed compulsion response (FCR), distance 2N, amount 1, standard $\frac{1}{\sqrt{2}}$ and a low-slung permit filter. From filter *w* outline four FIR filters of length 2*N* and of norm 1 equipped as unprotected in Figure 3 [25]–[27].

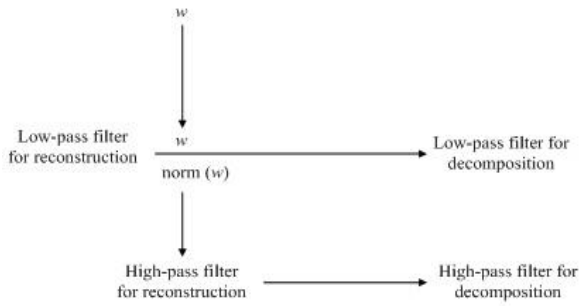

Figure 3. How to compute four filters

Assumed a signal s of distance N the detached wavelet adapts comprises of $\log_2 N$ periods at highest. Inaugural since s, the first step harvests two sets of dimensions: approximation amounts cA_1 and feature numbers cD_1. These trajectories are prolonged by convolvings through the low-pass strainer for calculation and with the high-pass strainer for feature are monitored by dyadic devastation. Additional accurately the first step is shown in Figure 4 [28], [29].

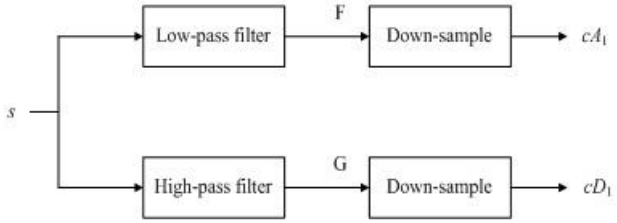

Figure 4. First phase of discrete wavelet transform

The extent of every strainer is identical to 2L. The product of convolving a dimension N indicator with a dimension 2L filter is N+2L–1. Hence, the indicators F and G are of measurement N+2L–1. Later down-selection by 2, the constant vectors cA_1 and cD_1 are of length $\left\lfloor \frac{N-1}{2} + L \right\rfloor$. Then succeeding step splits the calculation numbers cA_1 in two portions consuming the same arrangement transaction s by cA_1 and manufacturing cA_2 and cD_2 which displays in Figure 5 [30], [31].

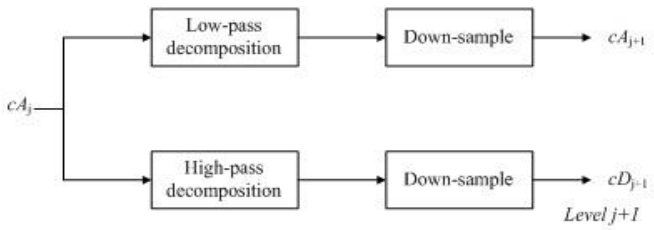

Figure 5. 1-D separate wavelet transform for disintegration stage

Equally, preliminary from cA_j and cD_j the opposite disconnected wavelet convert renovates cA_{j-1}, upsetting the decomposition phase through implanting zeros and convolving the consequences by the rebuilding filters [32]. Figure 6 shows the renovation step of 1-D separate wavelet transform.

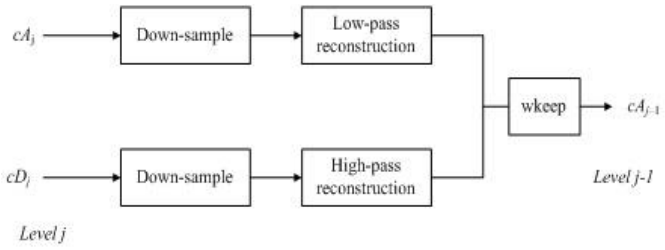

Figure 6. 1-D discrete wavelet transform for renovation phase

On behalf of images, a comparable algorithm is conceivable for 2-D wavelets and ascending meanings increased after 1-D wavelets by tensorial construction. This generous of 2-D discrete wavelet converts indications to a putrefaction of estimate quantities at equal *j* in four workings: the evaluation at level *j*+1 and the details in three alignments such as straight, upright and diagonal [33]. The discrete wavelet transmute of a discrete signal $X = [x[0], \dots, x[N-1]]^T$ is the process of getting the coefficients as in (4) and (5) [34].

$$W_\varphi[j_0, k] = \frac{1}{\sqrt{N}} \sum_{m=0}^{N-1} x[m] \varphi_{j_0,k}[m] = \frac{1}{\sqrt{N}} \sum_{m=0}^{N-1} x[m] 2^{j_0/2} \varphi[2^{j_0} m - k], \forall_k \quad (4)$$

$$W_\Psi[j, k] = \frac{1}{\sqrt{N}} \sum_{m=0}^{N-1} x[m] \Psi_{j,k}[m] = \frac{1}{\sqrt{N}} \sum_{m=0}^{N-1} x[m] 2^{j/2} \Psi[2^j m - k], \forall_k \; and \; all \; j > j_0 \quad (5)$$

While the source scaling and wavelet meanings are correspondingly formulated in (6) as monitors [35].

$$\begin{cases} \varphi_{j,k}[m] = 2^{j/2} \varphi[2^j m - k] \\ \Psi_{j,k}[m] = 2^{j/2} \Psi[2^j m - k] \end{cases} \quad (6)$$

Remember that both the scrabbling and wavelet meanings can be prolonged in terms of basis mounting purposes of the next higher purpose which shows in (7) as [35], [36].

$$\begin{cases} \varphi[m] = \sum_l h_\varphi[l] \sqrt{2} \varphi[2m - l] \\ \Psi[m] = \sum_l h_\Psi[l] \sqrt{2} \varphi[2m - l] \end{cases} \quad (7)$$

Currently seeing the algorithm as a wild origination to get the constants $W_\varphi[j, k]$ and $W_\Psi[j, k]$ of different scales *j*. Consider first the climbing function $\varphi[m]$. Trading *m* by $2^j m - k$ (scaled by 2^j and decrypted by *k*), then the mounting function develops like in (8) [37], [38].

$$\varphi[2^j m - k] = \sum_l h_\varphi[l] \sqrt{2} \varphi[2(2^j m - k) - l] = \sum_l h_\varphi[l] \sqrt{2} \varphi[2^{j+1} m - 2k - l] \quad (8)$$

Now the replacement of *n=2k+l and l=n-2k*, then (8) becomes just as (9) [38].

$$\varphi[2^j m - k] = \sum_n h_\varphi[n - 2k] \sqrt{2} \varphi[2^{j+1} m - n] \quad (9)$$

Likewise, the wavelet purpose can also be long-drawn-out just as in (10) [39].

$$\Psi[2^j m - k] = \sum_n h_\Psi[n - 2k] \sqrt{2} \varphi[2^{j+1} m - n] \quad (10)$$

This wavelet purpose which labeled in (10) is indistinguishable to the unique secondhand in comparison 5. So, supernumerary (10) into (5) then it converts like (11) [40].

$$W_\Psi[j, k] : \frac{1}{\sqrt{N}} \sum_{m=0}^{N-1} x[m] 2^{\frac{j}{2}} \Psi[2^j m - k] = \frac{1}{\sqrt{N}} \sum_{m=0}^{N-1} x[m] 2^{\frac{j}{2}} \left[\sum_n h_\Psi[n - 2k] \sqrt{2} \varphi[2^{j+1} m - n] \right]$$
$$: \sum_n h_\Psi[n - 2k] \left[\frac{1}{\sqrt{N}} \sum_{m=0}^{N-1} x[m] 2^{(j+1)/2} \varphi(2^{j+1} m - n) \right] \quad (11)$$

The appearance $\frac{1}{\sqrt{N}}\sum_{m=0}^{N-1} x[m]2^{(j+1)/2}\varphi(2^{j+1}m-n)$ materializes to be the wavelet change for the quantity of scale *j+1* in (12) [41].

$$W_\Psi[j+1,k] = \frac{1}{\sqrt{N}}\sum_{m=0}^{N-1} x[m]2^{(j+1)/2}\varphi(2^{j+1}m-n) \quad (12)$$

Consequently, a recursive relation among the wavelet transforms constants of two uninterrupted scale heights *j* and *j+1* shown in (13) and the similar is true to the mounting meaning which is also exposed in (14) [39]–[41].

$$W_\Psi[j,k] = \sum_n h_\Psi[n-2k]W_\Psi[j+1,n] \quad (13)$$

$$W_\varphi[j,k] = \sum_n h_\varphi[n-2k]W_\varphi[j+1,n] \quad (14)$$

Once associating (13) and (14) with a discrete difficulty then we get the consequence as a form of (15) as [42]–[44].

$$y[k] = h[k] * x[k] = \sum_n h[k-n]x[n] \quad (15)$$

Accordingly, the wavelet renovate constants $W_\varphi[j,k]$ and $W_\Psi[j,k]$ at the j^{th} scale canister stand attained from the quantities $W_\varphi[j+1,k]$ and $W_\Psi[j+1,k]$ at the $(j+1)^{th}$ scale by two belongings such as complication with time reversed h_φ or h_Ψ and sub-sampling to get every other illustrations in the convolution. Therefore, wavelet transmute and scaling meaning will become the shape as given in (16) as [45], [46].

$$\begin{cases} W_\Psi[j,k] = h_\Psi[-n] * W_\varphi[j+1,n]|_{n=2k,k\le 0} \\ W_\varphi[j,k] = h_\varphi[-n] * W_\varphi[j+1,n]|_{n=2k,k\le 0} \end{cases} \quad (16)$$

Created on (16), all wavelet then scrabbling numbers $W_\Psi[j,k]$ and $W_\varphi[j,k]$ of a agreed indication *X* can be gotten recursively from the constants $W_\Psi[J,k]$ and $W_\varphi[j,k]$ at the highest determination level *j=J* with all concentrated information and the *N* data points $x[m]$ $(m=0,\dots,N-1)$straight tried after the signal $x(t)$. As an associate of space V_J, these separate samples can be written as a rectilinear mixture of the climbing source purposes $\varphi_{J,k}[m]$ which shows in (17) as [47], [48]. Figure 7 present wavelet transform.

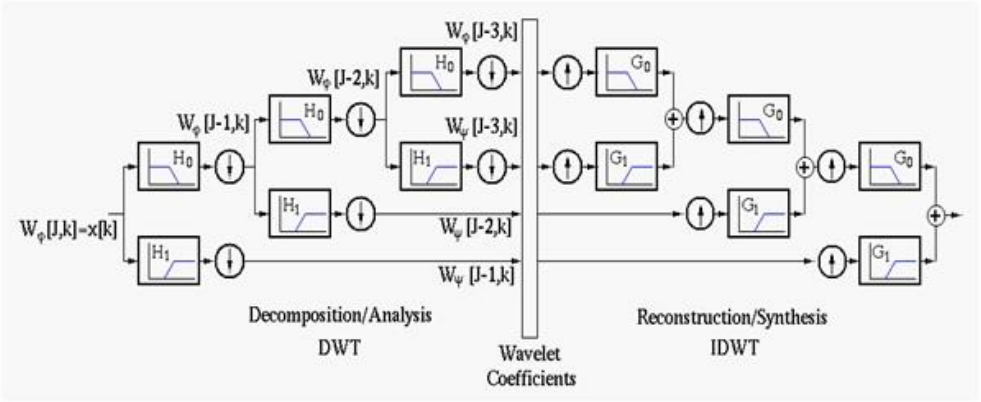

Figure 7. Diagram of fast wavelet transform with its operational [49]

2.3. Gabor filter

In image processing a Gabor filter is a linear filter used for texture analysis. As a linear filter, it reflects the account as monitors:

$$Process[(time\ varying\ input\ signals) \rightarrow (output\ signals)]\ \text{Subject to linearity}$$

Where linearity is a stuff which revenues that it can be explicitly characterized as a traditional line. Conferring to the linear function *f(x)* that function must indulges the two effects. First property is the conserving stuff as $\{f(x+y)=f(x)+f(y)\}$ and the second is equality of degree 1 which is $\{f(ax)=af(x), \forall\, a\}$ [38]. It mostly scrutinizes whether nearby any explicit regularity pleased trendy the pictures in plain directives in a constrained division everywhere the theme or pitch of investigation. In the latitudinal area, a 2D Gabor filter is a Gaussian Kernel function altered by a sinusoidal plane wave. Its impulse response is well-defined by a sinusoidal wave which augmented by a Gaussian function [50], [51]. Owing to the development intricacy stuff, the transformation of a Gabor filter's obligation rejoinder is the convolution of the choral determination which is identified as sinusoidal meaning and the Gaussian function. The filter has a material and a make-believe essential on behalf of orthogonal remits [52], [53]. These two workings may be designed into a multifarious number or used independently. As a complex method of Gabor filter is exposed in Equivalence 18 as:

$$g(x,y;\,\lambda,\theta,\Psi,\sigma,\gamma)=exp\left(-\frac{\acute{x}^2+\gamma^2\acute{y}^2}{2\sigma^2}\right)exp\left(i\left(2\pi\frac{\acute{x}}{\lambda}+\Psi\right)\right) \tag{17}$$

Material and invented parts of (18) revealed in (19) as:

$$\begin{cases} g(x,y;\,\lambda,\theta,\Psi,\sigma,\gamma)=\ exp\left(-\frac{\acute{x}^2+\gamma^2\acute{y}^2}{2\sigma^2}\right)\cos\left(2\pi\frac{\acute{x}}{\lambda}+\Psi\right), Real\ part \\ g(x,y;\,\lambda,\theta,\Psi,\sigma,\gamma)=\ exp\left(-\frac{\acute{x}^2+\gamma^2\acute{y}^2}{2\sigma^2}\right)\sin\left(2\pi\frac{\acute{x}}{\lambda}+\Psi\right)\ Imaginary\ part \end{cases} \tag{18}$$

Where:
- $x' = x\cos\theta + y\sin\theta$ and $y' = y\cos\theta - x\sin\theta$ are the components
- λ Characterizes the wavelength of the sinusoidal inspiration
- θ Denotes the alignment of the usual to the equivalent stripes of a Gabor meaning
- ψ is the stage offset, σ is the standard deviation of the Gaussian covering
- γ is the longitudinal facet relation and requires the ellipticity of the sustenance of the Gabor function

A fixed of Gabor filters with diverse occurrences and bearings can stay cooperative aimed at excavating convenient structures after an image (Haghighat *et al*., 2013). In the distinct field, 2D Gabor filters are given by [54], [55].

$$\begin{cases} G_c[i,j]=Be^{-\frac{(i^2+j^2)}{2\sigma^2}}\cos\left(2\pi f(i\cos\theta+j\sin\theta)\right) \\ G_s[i,j]=Ce^{-\frac{(i^2+j^2)}{2\sigma^2}}\sin\left(2\pi f(i\cos\theta+j\sin\theta)\right) \end{cases} \tag{19}$$

Where *B* and *C* are regulating factors to be determined, *f* defines the frequency. By changing θ is used for consistency orientation in a certain bearing while through the variation of$n$, dissimilarity [56]–[58].

3. EXPERIMENTAL RESULTS AND COMPARISON

Assessing these presentations of biometric technique is a problematic production. For the determination of judgment; we contrivance these approaches interpretation to the reproduced documents. To assistant their recital, we cast-off three categories of statistics which are UBIRIS, CASIA, and MMU. Iris database covers 280 eye images from 28 objects and each person has 10 images of eye. Altogether hearings were achieved by MATLAB version R2010b on the core processor. We use the usual technique to generate and normalize iris extents and use the amalgamation of three methods acknowledged overhead to mine the quantity. Consequently, we individual inspect and companion the exactness and computational application of chin extraction. Subsequently piece construct, we usage hybrid classifier for corresponding period (i.e) hard-to-test faults (HTTF) and false acceptance rate (FAR)/false rejection rate (FRR) are used for appraising the outcome.

4. ACCURACY RATE OF PREPROCESS SECTION

The precision of the planned technique is charted in Table 1 shows that the algorithm mechanism well even with the retinal images with complaints. From Table 1, Table 2 and Figure 8 consequence the result of preprocess constructed on the result the offered hybrid algorithm brand enhancements in the

preprocess segment. The development involve of changed dataset like UBIRIS, CASIA, MMU the development result show that the anticipated technique upgrading in the preprocess sector also.

Table 1. Preprocess of different data set result

Database	Total Images	Extracted successfully	Accuracy (%)
UBIRIS	280	97%	98.5%
CASIA	550	98%	98.9%
MMU	450	99%	99%

Table 2. Preprocess result of all technique

Database	Total images	Extracted successfully	Accuracy (%)
ANN	280	97%	98.5%
Block sum algorithm	550	98%	98.9%
SVM	450	99%	99%
Proposed technique			

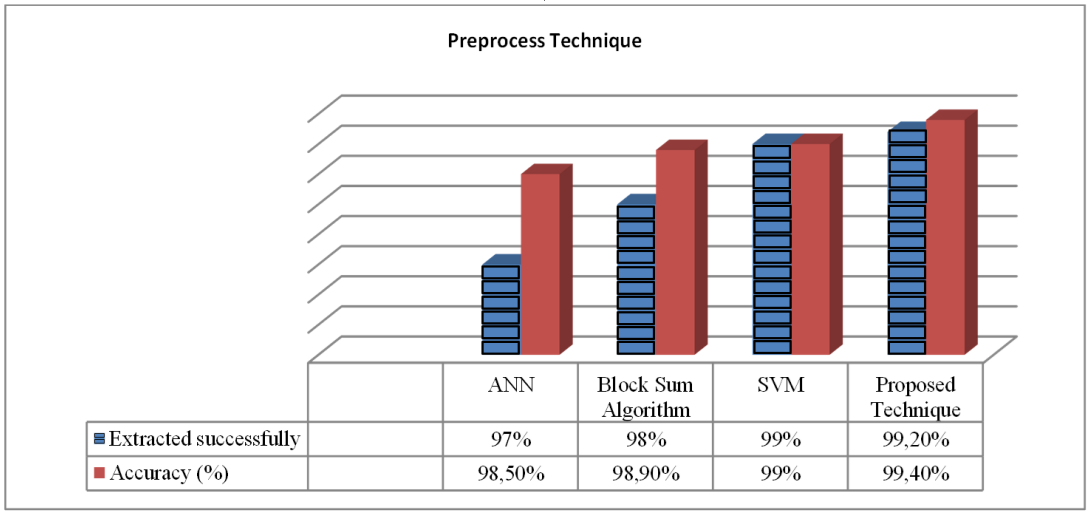

Figure 8. Overall result of preprocess

Table 3. Experimental results

Technique name	FAR/ FRR	Overall accuracy rate
ANN	4/6	97%
Block sum algorithm	3.2/3.1	97.5%
SVM	3/4	98%
Proposed technique	6/5	98.2%

False acceptance rate (FAR): is the possibility of the organization which imperfectly matches the input image with the no matching prototype in the database. It plaid the improper image in the database in situation of assessment gage, gamble the individual is pretender in actual then the identical notch is multifaceted than inception besides he is saline as unassuming that increases the FAR plus hereafter the recital similarly be contingent upon the variety of inception rate.

False dismissal rate (FRR): The position that the scheme plunges to extricate a contest amongst the effort outline and a different decoration in the record. It arrangements the out of a hundred of effective involvements which are wrongly rejected. Table 4 and Figure 9 show the result rendering to the result the suggested technique 98.20% overall result of the IRIS recognition as associate to the other algorithms.

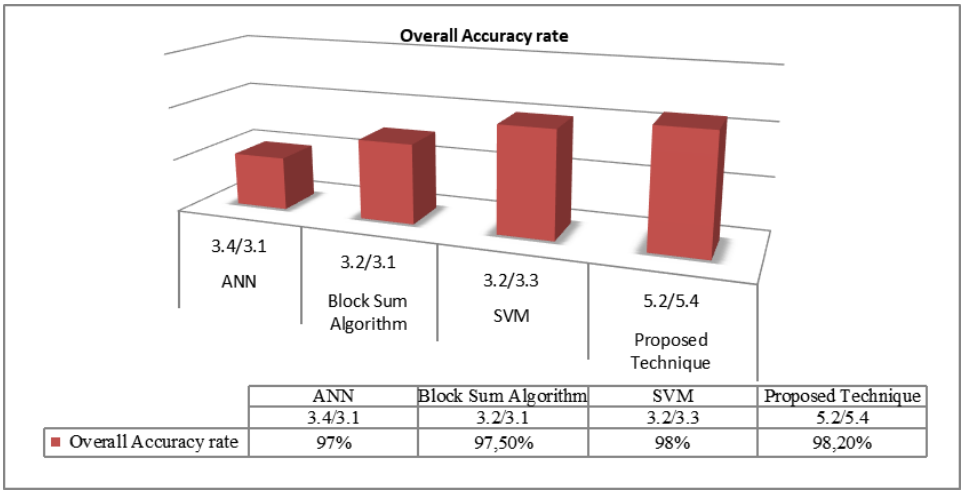

Figure 9. Over all result

5. CONCLUSION

In this article, we have debated feature abstraction and classifier of iris recognition by hybrid algorithm. The system be contingent largely on two stages, iris preprocess and iris classifier method. We need logical those transform preceding the iris pictures for encounter obtainable the appreciation proportion and exactitude. Outcomes of this test have publicized that the truthfulness in acknowledgment by fusion procedure is improved than artificial neural network (ANN), block sum algorithm, and support-vector machine (SVM). Likewise Crossbreed classifier i.e. mixture of ANN and FAR/FRR stay cast-off for matching whicheternally image is predictable or rejected. FAR and FRR in section by individual numerous approaches equally revealed in beyond diagram. Therefore, the planned process offers improved precision and appreciation amount those relative systems.

REFERENCES

[1] D. P. Ismi and M. Murinto, "Clustering based feature selection using partitioning around medoids (PAM)," *Jurnal Informatika*, vol. 14, no. 2, p. 50, May 2020, doi: 10.26555/jifo.v14i2.a17620.

[2] T. Krachenfels, H. Lohrke, J.-P. Seifert, E. Dietz, S. Frohmann, and H.-W. Hübers, "Evaluation of low-cost thermal laser stimulation for data extraction and key readout," *Journal of Hardware and Systems Security*, vol. 4, no. 1, pp. 24–33, Mar. 2020, doi: 10.1007/s41635-019-00083-9.

[3] V. R. Ayyagari, F. Boughorbel, A. Koschan, B. Abidi, and M. A. Abidi, "A pose invariant 3D face recognition method," 2005.

[4] G. Petmezas *et al.*, "Automated atrial fibrillation detection using a hybrid CNN-LSTM network on imbalanced ECG datasets," *Biomedical Signal Processing and Control*, vol. 63, p. 102194, Jan. 2021, doi: 10.1016/j.bspc.2020.102194.

[5] G. A. Papakostas, Y. S. Boutalis, D. A. Karras, and B. G. Mertzios, "Pattern classification by using improved wavelet compressed Zernike moments," *Applied Mathematics and Computation*, vol. 212, no. 1, pp. 162–176, Jun. 2009, doi: 10.1016/j.amc.2009.02.029.

[6] B. Leistedt, J. D. McEwen, P. Vandergheynst, and Y. Wiaux, "S2LET: a code to perform fast wavelet analysis on the sphere," *Astronomy and Astrophysics*, vol. 558, pp. 1–10, 2013, doi: 10.1051/0004-6361/201220729.

[7] B. Alhnaity, S. Kollias, G. Leontidis, S. Jiang, B. Schamp, and S. Pearson, "An autoencoder wavelet based deep neural network with attention mechanism for multi-step prediction of plant growth," *Information Sciences*, vol. 560, pp. 35–50, 2021, doi: 10.1016/j.ins.2021.01.037.

[8] K. Kozlov, E. Myasnikova, A. Pisareva, M. Samsonova, and J. Reinitz, "A method for two-dimensional registration and construction of the two-dimensional atlas of gene expression patterns in Situ," *In Silico Biology*, vol. 2, no. 2, pp. 125–141, 2002.

[9] R. Gad *et al.*, "Iris recognition using multi-algorithmic approaches for cognitive internet of things (CIoT) framework," *Future Generation Computer Systems*, vol. 89, pp. 178–191, Dec. 2018, doi: 10.1016/j.future.2018.06.020.

[10] M. A. M. Abdullah, S. S. Dlay, W. L. Woo, and J. A. Chambers, "Robust iris segmentation method based on a new active contour force with a noncircular normalization," *IEEE Transactions on Systems, Man, and Cybernetics: Systems*, vol. 47, no. 12, pp. 3128–3141, Dec. 2017, doi: 10.1109/TSMC.2016.2562500.

[11] E. M. Laadissi, J. Khalfi, F. Belhora, C. Ennawaoui, and A. El Ballouti, "Aging study of a lead-acid storage bank in a multi-source hybrid system," *Indonesian Journal of Electrical Engineering and Computer Science*, vol. 20, no. 3, pp. 1109–1117, Dec. 2020, doi: 10.11591/ijeecs.v20.i3.pp1109-1117.

[12] A. K. Gowda, A. B. Jayachandra, R. M. Lingaraju, and V. D. Rajkumar, "Novel approach for hybrid MAC scheme for balanced energy and transmission in sensor devices," *International Journal of Electrical and Computer Engineering*, vol. 12, no. 1, pp. 1003–1010, Feb. 2022, doi: 10.11591/ijece.v12i1.pp1003-1010.

[13] S. Saifullah, Y. Fauziyah, and A. S. Aribowo, "Comparison of machine learning for sentiment analysis in detecting anxiety based on social media data," *Jurnal Informatika*, vol. 15, no. 1, p. 45, Feb. 2021, doi: 10.26555/jifo.v15i1.a20111.

[14] K. K. Ashok, P. Dananjayan, and K. R. Vanga, "Low latency NoC switch using modified distributed round Robin arbiter," *Journal of Engineering Science and Technology Review*, vol. 14, no. 3, pp. 76–84, 2021, doi: 10.25103/jestr.143.09.

[15] T. Lu and A. Dooms, "Bayesian damage recognition in document images based on a joint global and local homogeneity model,"

Pattern Recognition, vol. 118, p. 108034, Oct. 2021, doi: 10.1016/j.patcog.2021.108034.
[16] S. Saini, D. Gupta, R. Ranjan Jha, G. Jaswal, and A. Nigam, "Iris segmentation in the wild using encoder-decoder-based deep learning techniques," in *AI and Deep Learning in Biometric Security*, 1st ed., Boca Raton, Florida: CRC Press, 2021, pp. 283–311.
[17] A. Singh, G. Jaswal, and A. Nigam, "Cancelable biometrics for template protection: future directives with deep learning," in *AI and Deep Learning in Biometric Security*, 1st ed., Boca Raton, Florida: CRC Press, 2021, pp. 23–49.
[18] G. V. Gopal and G. R. M. Babu, "An ensemble feature selection approach using hybrid kernel based SVM for network intrusion detection system," *Indonesian Journal of Electrical Engineering and Computer Science*, vol. 23, no. 1, pp. 558–565, Jul. 2021, doi: 10.11591/ijeecs.v23.i1.pp558-565.
[19] I. Bessadet, H. Tédjini, and I. K. Bousserhane, "Hydrogen electrified railways based shunt hybrid filter," *Indonesian Journal of Electrical Engineering and Computer Science*, vol. 21, no. 3, pp. 1291–1298, Mar. 2021, doi: 10.11591/ijeecs.v21.i3.pp1291-1298.
[20] A. Ullah and N. M. Nawi, "An improved in tasks allocation system for virtual machines in cloud computing using HBAC algorithm," *Journal of Ambient Intelligence and Humanized Computing*, pp. 1–14, Oct. 2021, doi: 10.1007/s12652-021-03496-z.
[21] S. Ouhame, Y. Hadi, and A. Ullah, "An efficient forecasting approach for resource utilization in cloud data center using CNN-LSTM model," *Neural Computing and Applications*, vol. 33, no. 16, pp. 10043–10055, Aug. 2021, doi: 10.1007/s00521-021-05770-9.
[22] D. Kumalasari, A. B. W. Putra, and A. F. O. Gaffar, "Speech classification using combination virtual center of gravity and k-means clustering based on audio feature extraction," *Jurnal Informatika*, vol. 14, no. 2, p. 85, May 2020, doi: 10.26555/jifo.v14i2.a17390.
[23] T. Dee, R. Scheel, N. Montelibano, and A. Tyagi, "User-silicon entangled mobile identity authentication," *Journal of Hardware and Systems Security*, vol. 4, no. 3, pp. 208–229, Sep. 2020, doi: 10.1007/s41635-020-00098-7.
[24] A. Rabie, K. El Shafie, A. Hammuoda, and M. Rohiem, "Data ecryption based on multi-order FrFT, and FPGA implementation of DES algorith," *International Journal of Reconfigurable and Embedded Systems (IJRES)*, vol. 9, no. 2, p. 141, Jul. 2020, doi: 10.11591/ijres.v9.i2.pp141-152.
[25] R. R. Jha, G. Jaswal, D. Gupta, S. Saini, and A. Nigam, "PixISegNet: pixel-level iris segmentation network using convolutional encoder- decoder with stacked hourglass bottleneck," *IET Biometrics*, vol. 9, no. 1, pp. 11–24, Jan. 2020, doi: 10.1049/iet-bmt.2019.0025.
[26] A. Noruzi, M. Mahlouji, and A. Shahidinejad, "Iris recognition in unconstrained environment on graphic processing units with CUDA," *Artificial Intelligence Review*, vol. 53, no. 5, pp. 3705–3729, Jun. 2020, doi: 10.1007/s10462-019-09776-7.
[27] Z. Garroussi, R. Ellaia, E. G. Talbi, and J. Y. Lucas, "A hybrid non-dominated sorting genetic algorithm for a multi-objective demand-side management problem in a smart building," *International Journal of Electrical and Computer Engineering*, vol. 10, no. 1, pp. 559–574, Feb. 2020, doi: 10.11591/ijece.v10i1.pp559-574.
[28] O. Zebraoui and M. Bouzi, "Improved MPPT controls for a standalone PV/wind/battery hybrid energy system," *International Journal of Power Electronics and Drive Systems*, vol. 11, no. 2, pp. 988–1001, Jun. 2020, doi: 10.11591/ijpeds.v11.i2.pp988-1001.
[29] M. A. S. Aboelela, "Application of optimal artificial intelligence based tuned controllers to a class of embedded nonlinear power system," *International Journal of Reconfigurable and Embedded Systems (IJRES)*, vol. 9, no. 1, p. 83, Mar. 2020, doi: 10.11591/ijres.v9.i1.pp83-92.
[30] A. Ullah and N. M. Nawi, "Enhancing the dynamic load balancing technique for cloud computing using HBATAABC algorithm," *International Journal of Modeling, Simulation, and Scientific Computing*, vol. 11, no. 5, p. 2050041, Oct. 2020, doi: 10.1142/S1793962320500415.
[31] C. Konstantinou and M. Maniatakos, "Hardware-layer intelligence collection for smart grid embedded systems," *Journal of Hardware and Systems Security*, vol. 3, no. 2, pp. 132–146, Jun. 2019, doi: 10.1007/s41635-018-0063-0.
[32] J. Hájek and M. Drahanský, "Recognition-based on eye biometrics: iris and retina," in *Biometric-Based Physical and Cybersecurity Systems*, M. S. Obaidat, I. Traore, and I. Woungang, Eds. Cham: Springer International Publishing, 2018, pp. 37–102.
[33] A. S. Leal and H. M. Paiva, "A new wavelet family for speckle noise reduction in medical ultrasound images," *Measurement*, vol. 140, pp. 572–581, Jul. 2019, doi: 10.1016/j.measurement.2019.03.050.
[34] P. Drozdowski, C. Rathgeb, and C. Busch, "Computational workload in biometric identification systems: an overview," *IET Biometrics*, vol. 8, no. 6, pp. 351–368, Nov. 2019, doi: 10.1049/iet-bmt.2019.0076.
[35] G. Mishra and R. Hegde, "Performance optimization of task intensive real time applications on multicore ECUs - a hybrid scheduler," *International Journal of Reconfigurable and Embedded Systems (IJRES)*, vol. 8, no. 2, p. 114, Jul. 2019, doi: 10.11591/ijres.v8.i2.pp114-123.
[36] A. Ullah, N. M. Nawi, J. Uddin, S. Baseer, and A. H. Rashed, "Artificial bee colony algorithm used for load balancing in cloud computing: review," *IAES International Journal of Artificial Intelligence*, vol. 8, no. 2, pp. 156–167, Jun. 2019, doi: 10.11591/ijai.v8.i2.pp156-167.
[37] W. Andre and O. Couillard, "Design and implementation of a new architecture of a real-time reconfigurable digital modulator (DM) into QPSK, 8-PSK, and 16-PSK on FPGA," *International Journal of Reconfigurable and Embedded Systems (IJRES)*, vol. 7, no. 3, pp. 173–185, Nov. 2018, doi: 10.11591/ijres.v7.i3.pp173-185.
[38] A. S. N. Nassar, "A hybrid multibiometric system for personal identification based on face and iris traits. The development of an automated computer system for the identification of humans by integrating facial and iris features using localization, feature extraction, hand," Ph.D. dissertation, Department of Electrical Engineering and Computer Science, University of Bradford, Bradford, England, 2018.
[39] Y. Alvarez-Betancourt and M. Garcia-Silvente, "A keypoints-based feature extraction method for iris recognition under variable image quality conditions," *Knowledge-Based Systems*, vol. 92, pp. 169–182, Jan. 2016, doi: 10.1016/j.knosys.2015.10.024.
[40] U. T. Tania, "Development of an IRIS authentication algorithm for personal identification," M.S. thesis, Department of Computer and Information Engineering, International Islamic University Malaysia, Kuala Lumpur, Malaysia, 2015.
[41] H. M. Sim, H. Asmuni, R. Hassan, and R. M. Othman, "Multimodal biometrics: weighted score level fusion based on non-ideal iris and face images," *Expert Systems with Applications*, vol. 41, no. 11, pp. 5390–5404, Sep. 2014, doi: 10.1016/j.eswa.2014.02.051.
[42] K. K. Shukla and A. K. Tiwari, *Efficient algorithms for discrete wavelet transform: with applications to denoising and fuzzy inference systems*. Cham: Springer Nature, 2013.
[43] K. Fatima Sharif and S. N. Biswas, "6 transistors and 1 memristor based memory Cell," *International Journal of Reconfigurable*

and Embedded Systems (IJRES), vol. 9, no. 1, p. 42, Mar. 2020, doi: 10.11591/ijres.v9.i1.pp42-51.
[44] A. Abbate, C. M. DeCusatis, and P. K. Das, *Wavelets and subbands: fundamentals and applications*. Cham: Springe Nature, 2012.
[45] A. Katunin, "Damage identification in composite plates using two-dimensional B-spline wavelets," *Mechanical Systems and Signal Processing*, vol. 25, no. 8, pp. 3153–3167, Nov. 2011, doi: 10.1016/j.ymssp.2011.05.015.
[46] J.-L. Starck, F. Murtagh, and J. Fadili, *Sparse image and signal processing: wavelets, curvelets, morphological diversity*. Cambridge: Cambridge University Press, 2010.
[47] T. S. Li, "Applying wavelets transform and support vector machine for copper clad laminate defects classification," *Computers and Industrial Engineering*, vol. 56, no. 3, pp. 1154–1168, Apr. 2009, doi: 10.1016/j.cie.2008.09.018.
[48] B. Yin, X. Li, Y. Shi, F. Zhang, and N. Zhang, "Directional lifting-based wavelet transform for multiple description image coding," *Signal Processing: Image Communication*, vol. 23, no. 1, pp. 42–57, Jan. 2008, doi: 10.1016/j.image.2007.10.001.
[49] H. Aznaoui, A. Ullah, S. Raghay, L. Aziz, and M. H. Khan, "An efficient GAF routing protocol using an optimized weighted sum model in WSN," *Indonesian Journal of Electrical Engineering and Computer Science*, vol. 22, no. 1, pp. 396–406, Apr. 2021, doi: 10.11591/ijeecs.v22.i1.pp396-406.
[50] A. Hanane, A. Ullah, and S. Raghay, "Enhanced GAF protocol based on graph theory to optimize energy efficiency and lifetime in WSN technology," *International Journal of Intelligent Unmanned Systems*, Dec. 2021, doi: 10.1108/IJIUS-08-2021-0096.
[51] B. K. Alsberg, A. M. Woodward, and D. B. Kell, "An introduction to wavelet transforms for chemometricians: a time- frequency approach," *Chemometrics and Intelligent Laboratory Systems*, vol. 37, no. 2, pp. 215–239, Jun. 1997, doi: 10.1016/S0169-7439(97)00029-4.
[52] M. Farge, "Wavelet transforms and their applications to turbulence," *Annual review of fluid mechanics*, vol. 24, no. 1, pp. 395–458, 1992.
[53] J. Morlet, G. Arens, E. Fourgeau, and D. Glard, "Wave propagation and sampling theory—part I: complex signal and scattering in multilayered media," *GEOPHYSICS*, vol. 47, no. 2, pp. 203–221, Feb. 1982, doi: 10.1190/1.1441328.
[54] N. Hamad and K. Taouil, "Exploring wavelets subband decomposition toward a computer aided detection of microcalcification in breast cancer," in *The 2nd International Conference on Distributed Frameworks for Multimedia Applications*, May 2006, pp. 1–8, doi: 10.1109/DFMA.2006.296920.
[55] I. Nurhaida, R. Manurung, and A. M. Arymurthy, "Performance comparison analysis features extraction methods for batik recognition," in *2012 International Conference on Advanced Computer Science and Information Systems, ICACSIS 2012-Proceedings*, 2012, pp. 207–212.
[56] T. Alam, A. Ullah, and M. Benaida, "Deep reinforcement learning approach for computation offloading in blockchain-enabled communications systems," *Journal of Ambient Intelligence and Humanized Computing*, Jan. 2022, doi: 10.1007/s12652-021-03663-2.
[57] A. Ullah, N. M. Nawi, M. Aamir, A. Shazad, and S. N. Faisal, "An improved multi-layer cooperation routing in visual sensor network for energy minimization," *International Journal on Advanced Science, Engineering and Information Technology*, vol. 9, no. 2, pp. 664–670, Mar. 2019, doi: 10.18517/ijaseit.9.2.2957.
[58] Arifullah, S. Baseer, and S. Umar, "Role of cooperation in energy minimization in visual sensor network," in *2016 6th International Conference on Innovative Computing Technology, INTECH 2016*, Aug. 2017, pp. 447–452, doi: 10.1109/INTECH.2016.7845026.

BIOGRAPHIES OF AUTHORS

Arif Ullah He received the B.Sc. Degree in Computer Science from University of Peshawar, Pakistan, in 2009, the M.Sc. Degree in Computer Science university of Peshawar, Pakistan, in 2012, the MS Computer Science from University of Agriculture Pakistan in 2016 and Ph.D. Degree in Information Technology from Universiti Tun Hussein Onn Malaysia in Malaysia 2021. His Research background of cloud computing, IoT, Deep Learning, optimization and WSN. He can be contacted at email: Arifullahms88@gmail.com.

Abdu Salam working as an Assistant Professor at the Department of Computer Science Abdul Wali Khan University. His Research background of cloud computing, IoT, Deep Learning, optimization and WSN. He can be contacted at email: abdusalam@awkum.edu.pk.

Hanane El Raoui working as researcher at 3Department of Computer Science and Artificial Intelligence, Universidad de Granada, 18014 Granada, Spain. Research background of cloud Security, IoT, Deep Learning, optimization and WSN along with optimization technique. She can be contacted at email: hanane.elraoui@uir.ac.ma.

Dorsaf Sebai holds the Engineering Degree in Computer Networks and Telecommunications from National Institute of Applied Sciences and Technologies (INSAT - Tunisia), the Master Degree in Electronic Systems and Communication Networks from Tunisia Polytechnic School (EPT - Tunisia) and the Thesis Degree in Computer Science from National School of Computer Sciences (ENSI - Tunisia). From 2009 to 2016, she joined INSAT then the Higher Institute of Computer Science and Management (ISIGK - Kairouan) as Assistant. Since 2017, she has held the position of Assistant Professor at INSAT., She can be contacted at email: dorsaf.sebai@ensi-uma.tn.

Mahnaz Rafie received the B.Sc. Degree in Computer Engineering from Allameh Mohaddese Noori Institute of Higher Education, Iran, in 2006, the M.Sc. Degree in Computer Architecture from Islamic Azad University of Arak in 2011, the Ph.D. Degree in Computer Architecture at Department of Computer Engineering, Science and Research Branch, Islamic Azad University, Tehran, Iran, in 2016. She can be contacted at email: m.rafie@srbiau.ac.ir.